

# Optimal Torque Allocation for All-Wheel-Drive Electric Vehicles Using a Reinforcement Learning Algorithm

Reza Jafari

*School of Physics, Engineering  
and Computer Science  
University of Hertfordshire  
Hatfield AL10 9AB, UK  
r.jafari@herts.ac.uk*

Pouria Sarhadi

*School of Physics, Engineering  
and Computer Science  
University of Hertfordshire  
Hatfield AL10 9AB, UK  
p.sarhadi@herts.ac.uk*

Amin Paykani

*School of Engineering  
and Materials Science  
Queen Mary University of London  
London E1 4NS, UK  
a.paykani@qmul.ac.uk*

Shady S. Refaat

*School of Physics, Engineering  
and Computer Science  
University of Hertfordshire  
Hatfield AL10 9AB, UK  
s.khalil3@herts.ac.uk*

Pedram Asef

*Advanced Propulsion Laboratory  
Department of Mechanical Engineering  
University College London  
London WC1E 6BT, UK  
pedram.asef@ucl.ac.uk*

**Abstract**—A novel reinforcement learning-based algorithm is proposed in this paper for the optimal torque allocation among the four wheels of an all-wheel-drive (AWD) electric vehicle (EV) through a direct yaw moment control approach. A hierarchical structure was utilized for the control procedure, in which a linear quadratic regulator (LQR) controller is exploited for the high-level controller to generate yaw moments and a novel deep deterministic policy gradient (DDPG) algorithm is employed for the low-level controller. The DDPG agent possesses the ability to interact with the environment and learn to optimally split torque among four wheels. The vehicle is modeled via a nonlinear model with seven degrees of freedom (7 DOF), while the reference signals are generated by a bicycle model with two degrees of freedom (2 DOF). For enhanced precision in vehicle modeling, the tire model is characterized by the Pacejka Magic Formula (MF), which offers a rigorous and empirically validated representation of tire behavior. The proposed model is verified through a scenario of the response of the vehicle while circumnavigating a curve on a slippery road. The obtained results depict improved performance and enhanced dynamic stability compared to the conventional model with the average torque distribution method. Control over the yaw behavior and increased dynamic stability are achieved, while the understeer and oversteer are avoided.

**Index Terms**—Direct yaw control, Electric vehicle, Reinforcement learning, Torque vectoring, Vehicle dynamics

## I. INTRODUCTION

The trend towards the eradication of fossil fuels and obtaining sustainable resources has attracted much attention in recent years [1]–[3]. The surge in electric vehicle (EV) adoption marks a shift towards sustainable transportation and the elimination of internal combustion engines (ICEs) with EVs leading the charge due to their efficiency and low emissions. The exploitation of electrical machines (EMs), as the heart of EVs, has provided the opportunity, especially for EVs with

the all-wheel drive (AWD) architecture, to take advantage of improved dynamic stability owing to the control in distributing torque among all wheels [4], [5].

Direct yaw control (DYC) stands as an effective improvement in the realm of advanced vehicle stability systems, primarily aimed at developing the stability and maneuverability of vehicles under various driving scenarios [6]. DYC systems can directly influence the yaw behavior of a vehicle, counteracting undesirable motions, such as understeer or oversteer [7], [8]. An intelligent torque vectoring (TV) approach was proposed in [9] based on a fuzzy approach to estimate vertical tire forces and control yaw moment. Torque values applied to the wheels were determined using a conventional method for average torque allocation, taking into account the required longitudinal and lateral torques. PID and LQR controllers were used for a TV approach [10], and both controllers have been tested for a Formula Student prototype. An integrated adaptive control strategy was proposed in [11] to increase the dynamics of a vehicle founded on DYC. A study was conducted in [12] on how to control the deviation in mass of the vehicle and tire-road friction coefficient. The low-level controller aimed to allocate braking torque in response to the additional yaw moment. In [13], a hierarchical control strategy was introduced, encompassing high-level and low-level controllers, with the goal of enhancing dynamic stability. This approach featured a torque allocation technique to address the issue of uniform torque distribution found in conventional average torque allocation methods. The design of the optimal torque allocation algorithm was centered around an objective function.

Even though plenty of research has focused on DYC enhancement, the development of a controller with the ability to adaptively learn from the driving environment remains an essential need. A reinforcement learning (RL)-based approach was presented in [14] to calculate a balanced coefficient between the energy consumption and stability of a vehicle. However, there is a requirement for an intelligent control approach for the optimal torque distribution across the four wheels.

This paper presents a novel method to provide the low-level controller with an intelligent-based torque distribution method exploiting a deep deterministic policy gradient (DDPG) algorithm. This RL-based approach promises to dynamically adapt torque distribution in real time, ensuring optimal vehicular stability and performance through continuous learning from the environment. The utilization of the intelligent low-level controller is an effective solution for handling complicated nonlinear interactions in AWD systems. Moreover, the unique learning capability of the DDPG agent allows for customization and fine-tuning to align with the characteristics of the vehicle. This work is structured as follows. Section II will delve into the DYC and model of the system, and Section III will introduce the active safety layer. The focus of Section IV will be on the RL-based method for torque allocation. The simulation outcomes will be discussed in Section V, with the conclusion outlined in Section VI.

## II. DIRECT YAW CONTROL AND SYSTEM MODEL

The enhancement of vehicular stability and maneuverability of a vehicle necessitates a sophisticated control approach and a model of the system to handle safety issues. For this aim, an active torque distribution method can be employed to independently apply different torque values to each wheel and control the traction of the vehicle.

### A. Torque vectoring framework

In this study, a feasible TV approach is implemented to boost the stability of an AWD EV. The TV framework is structured around a high-level controller designed to calculate the yaw moment and a low-level controller tasked with splitting the required torque among the four wheels of the vehicle. A linear quadratic regulator (LQR) controller is utilized for the high-level hierarchy to minimize a quadratic cost function. Additionally, an intricate representation of the dynamics of a vehicle is estimated using a nonlinear model that incorporates seven degrees of freedom (7 DOF), while the reference yaw rate and sideslip angle are derived from a two degrees of freedom (2 DOF) bicycle model.

### B. Nonlinear vehicle model with 7 DOF

A nonlinear model with 7 DOF is used to evaluate the performance of an AWD EV [15], as demonstrated in Fig. 1. The longitudinal velocity ( $V_x$ ), lateral velocity ( $V_y$ ), yaw

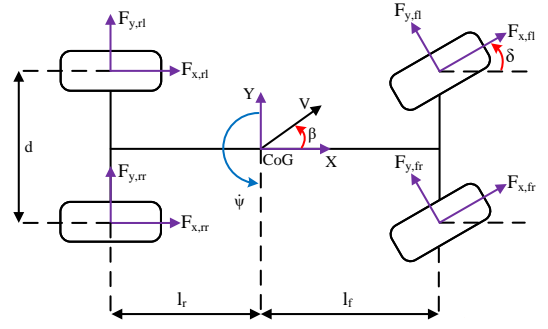


Fig. 1: Diagram of vehicle model with 7 DOF

TABLE I: VEHICLE DYNAMIC PARAMETERS OF THIS STUDY

Description	Unit	Value
Total mass of the vehicle	kg	1411
Vehicle yaw inertia	kg.m <sup>2</sup>	2031
Distance from COG to front axle	m	1.04
Distance from COG to rear axle	m	1.56
Wheel tread	m	1.48
Wheel radius	m	0.3
Cornering stiffness of tires	N/rad	45000
wheel inertia	kg.m <sup>2</sup>	1.46

rate ( $\dot{\psi}$ ), and the angular velocity of four wheels ( $\omega_{ij}$ ) are accounted for 7 DOF.

$$m(\dot{V}_x - \dot{\psi}V_y) = (F_{xfl} + F_{xfr}) \cos \delta - (F_{yfl} + F_{yfr}) \sin \delta + F_{xrl} + F_{xrr} \quad (1)$$

$$m(\dot{V}_y + \dot{\psi}V_x) = (F_{yfl} + F_{yfr}) \cos \delta + (F_{xfl} + F_{xfr}) \sin \delta + F_{yrl} + F_{yrr} \quad (2)$$

$$I_z \ddot{\psi} = \ell_f (F_{xfl} + F_{xfr}) \sin \delta + \ell_f (F_{yfl} + F_{yfr}) \cos \delta - \ell_r (F_{yrl} + F_{yrr}) + \frac{\ell_w}{2} (F_{xfr} - F_{xfl}) \cos \delta + \frac{\ell_w}{2} (F_{xrr} - F_{xrl}) + \frac{\ell_w}{2} (F_{yfl} - F_{yfr}) \sin \delta \quad (3)$$

$$I_w \dot{\omega}_{ij} = T_{ij} - F_{xij} R_w \quad (4)$$

where  $ij = \{fl, fr, rl, rr\}$  represent front-left, front-right, rear-left, and rear-right wheels.  $F_{xij}$  and  $F_{yij}$  are the longitudinal and lateral forces of four wheels, respectively.  $m$  is the total mass of the vehicle,  $\delta$  is the steering front wheel angle,  $R_w$  is the tire effective radius,  $I_z$  is the vehicle moment of inertia around the vertical axis,  $\ell_f$  is the distance between center of gravity (COG) and the front axle,  $\ell_r$  is the distance between COG and rear axle,  $\ell_w$  is the wheel tread,  $I_w$  is the wheel inertia, and  $T_{ij}$  is the torque of wheels. The magic formula (MF) is employed to model the complex behavior of tires. The vehicle parameters are tabulated in Table I.

### C. Bicycle model with 2 DOF

To generate the reference signals, a bicycle model is exploited with 2 DOF [16], [17], as depicted in Fig. 2.

$$\dot{\psi}_{des} = \frac{V_x}{L + K_{US}V_x^2} \delta \quad (5)$$

$$\beta_{des} = \frac{1}{L + K_{US}V_x^2} \left( \ell_r - \frac{\ell_f}{L} \frac{m}{2C_{\alpha r}} V_x^2 \right) \delta \quad (6)$$

where  $L$  is  $\ell_f + \ell_r$ ,  $C_{\alpha f}$  and  $C_{\alpha r}$  are the cornering stiffness of the front and rear tires, respectively.  $K_{US}$  is the understeer gradient, which is defined as:

$$K_{US} = \frac{m(\ell_r C_{\alpha r} - \ell_f C_{\alpha f})}{2C_{\alpha f} C_{\alpha r} L} \quad (7)$$

Nevertheless, the admissible range for the desired yaw rate is constrained by the tire-road friction coefficient, in which the desired yaw rate is subject to an upper limit:

$$\dot{\psi}_{limit} = 0.85 \frac{\mu g}{V_x} \quad (8)$$

Tires deviate from their linear characteristics and approach the adhesion limit at high sideslip angles. To avoid a large sideslip angle, an upper bound can be defined based on the following empirical expression:

$$\beta_{limit} = \tan^{-1}(0.02\mu g) \quad (9)$$

### III. ACTIVE SAFETY CONTROL LAYER

The active safety control of the torque vectoring system employs a dual-level control hierarchy to improve the dynamic stability of AWD EVs.

#### A. High-level controller

The LQR serves as the high-level controller to regulate the behavior of the dynamic system [18]. The desired system dynamics are captured by state-space representations. Therefore, the relationship between the additional yaw moment and the deviation of the motion can be expressed as:

$$\begin{bmatrix} \Delta \dot{\beta} \\ \Delta \dot{\psi} \end{bmatrix} = A \begin{bmatrix} \Delta \beta \\ \Delta \psi \end{bmatrix} + B^0 \Delta M_z \quad (10)$$

where  $\Delta \beta$  and  $\Delta \psi$  are the difference between the reference and actual sideslip angle and yaw rate, respectively.  $A$  and  $B^0$  are matrices to define the state space equation. The cost function is defined as:

$$J = \int_0^\infty (x^T Q x + u^T R u) dt \quad (11)$$

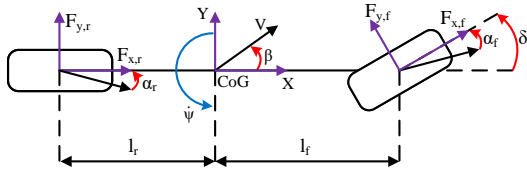


Fig. 2: Bicycle model with 2 DOF

The cost function aims to achieve a trade-off between the state values and the control effort by penalizing the state deviations and the control effort, represented by  $Q$  and  $R$ , respectively. The linear control law is defined as:

$$u = Kx \quad (12)$$

where

$$K = -R^{-1}B^T P \quad (13)$$

The high-level controller output can be determined through the following calculation:

$$M_z = Kx(t) = k_1(\beta - \beta_d) + k_2(\dot{\psi} - \dot{\psi}_d) \quad (14)$$

#### B. Low-level controller with average torque allocation method

The low-level controller aims to optimally split the torque across the four wheels of the AWD EV. The yaw moment calculated by the LQR controller is applied to a low-level controller to distribute torque among wheels based on the average distribution algorithm [19].

$$T_{fl} = \frac{R_w}{1 + \frac{1}{\rho_L}} \left( \frac{F_{x,t}}{2} - \frac{M_z}{\ell_w} \right) \quad (15)$$

$$T_{fr} = \frac{R_w}{1 + \frac{1}{\rho_R}} \left( \frac{F_{x,t}}{2} + \frac{M_z}{\ell_w} \right) \quad (16)$$

$$T_{rl} = \frac{R_w}{1 + \rho_L} \left( \frac{F_{x,t}}{2} - \frac{M_z}{\ell_w} \right) \quad (17)$$

$$T_{rr} = \frac{R_w}{1 + \rho_R} \left( \frac{F_{x,t}}{2} + \frac{M_z}{\ell_w} \right) \quad (18)$$

where  $M_z$  is the yaw moment, and  $F_{x,t}$  is the total demand force.  $\rho_R$  and  $\rho_L$  can be obtained as follows:

$$\rho_L = \frac{F_{z,fl}}{F_{z,rl}} \quad (19)$$

$$\rho_R = \frac{F_{z,fr}}{F_{z,rr}} \quad (20)$$

where  $F_{z,ij}$  are vertical tire forces.

### IV. REINFORCEMENT LEARNING-BASED TORQUE ALLOCATION METHOD

The reinforcement learning-based torque allocation method introduces a paradigm shift by applying optimal torque values to each wheel of the AWD EV through the utilization of a DDPG algorithm. This novel approach enables the system to learn optimal torque distribution policies directly from the interaction of the vehicle with its environment, allowing for real-time adaptation to varying road conditions and driving scenarios. Unlike traditional control methods, this RL-based system continuously improves its performance through trial and error, leading to a more intuitive and dynamic adaptation of torque distribution that enhances vehicle stability and maneuverability. The schematic of the proposed control algorithm is demonstrated in Fig. 3.

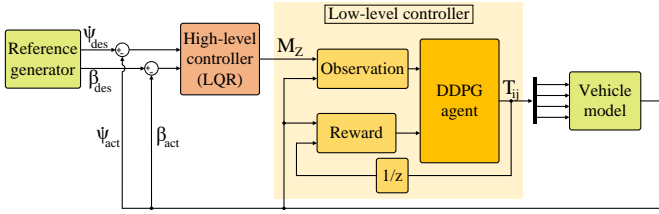


Fig. 3: Schematic of the proposed control structure

TABLE II: HYPERPARAMETER SETTINGS OF THE DDPG

Parameter	Value
Critic learn rate	1e-3
Actor learn rate	0.9e-4
Noise model	Ornstein Uhlenbeck (OU)
Noise option standard deviation	0.6
Variance decay rate	1e-5
Discount factor	0.99
Target smooth factor	1e-3
Mini batch size	64

The observation signals can be expressed as:

$$S_t = \{\dot{\psi}, \dot{\psi}_e, \int \dot{\psi}_e, \dot{\beta}, \dot{\beta}_e, \int \dot{\beta}_e, v_x, v_e, \int v_e, \omega_{ij}, s_{x,ij}, F_{x,total}, M_z\} \quad (21)$$

Four actions are known as the outputs of the DDPG agent:

$$a_t = \{T_{fl}, T_{fr}, T_{rl}, T_{rr}\} \quad (22)$$

The reward function has an impressive impact on the performance of the control algorithm, which can be defined as:

$$r_t(s_t, a_t) = R_1 + R_2 + R_3 + R_4 + R_5 \quad (23)$$

where  $R_1$  is a boolean term to guide the agent to make the yaw rate error less than a specific value:

$$R_1 = \begin{cases} w_1 & \text{if } |\dot{\psi}_e| \leq 0.0001 \text{ rad} \\ 0 & \text{otherwise} \end{cases} \quad (24)$$

where  $w_1$  is 4,  $w_2$  is 10,  $w_3$  is 2, and  $w_4$  is 1.  $R_2$ ,  $R_3$  and  $R_4$  are defined as:

$$R_2 = -w_2 * (\dot{\psi}_e)^2 \quad (25)$$

$$R_3 = -w_3 * (\beta_e)^2 \quad (26)$$

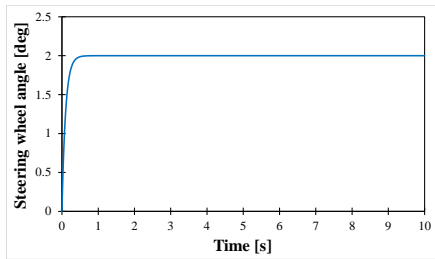


Fig. 4: Steering wheel angle

$$R_4 = -w_4 * (v_e)^2 \quad (27)$$

$R_5$  is defined to penalize the excessive control effort taken by the agent:

$$R_5 = -\Delta u(t)^T * w_5 * \Delta u(t) \quad (28)$$

where  $\Delta u(t)$  is  $[\Delta T_{fl}, \Delta T_{fr}, \Delta T_{rl}, \Delta T_{rr}]$  and  $w_4$  is  $\text{diag}(0.1, 0.1, 0.1, 0.1)_{4 \times 4}$ . The hyperparameter settings are summarised in Table. II.

## V. SIMULATION RESULTS

The performance of the proposed control algorithm can be assessed by implementing the scenario of applying a constant steering wheel angle as illustrated in Fig. 4. To test the applicability of the proposed control algorithm under challenging conditions that are likely to stress the vehicle dynamic stability, the scenario involves the vehicle traveling at a speed of 90 km/h on a snowy road, where the road adhesion coefficient is 0.2.

The results of the simulation are demonstrated in Fig. 5. As demonstrated in Fig. 5a, the proposed torque allocation method based on DDPG algorithms depicts an improved performance compared to the conventional one. Fig. 5b compares the sideslip angle of the novel DDPG algorithm and the conventional method. Fig. 5c shows the trajectory of the vehicle, in which the proposed method provides the vehicle with the capability to follow the desired path better than the conventional average torque allocation method. The AWD EV takes advantage of the proposed DDPG algorithm to obtain higher stability and maneuverability on a snowy road with slippery conditions. Fig. 5d demonstrates the lateral acceleration of the vehicle for the conventional and DDPG approaches. Finally, the wheel torques and angular velocities are illustrated in Fig. 5e and Fig. 5f, respectively. As shown, the proposed approach allocates the optimal torque to the wheels in favor of obtaining improved stability.

The RL agent demonstrates a remarkable ability to maintain vehicle stability, minimize sideslip angles, and adhere to the desired path, outperforming the traditional method. These results not only verify the effectiveness of the RL-based approach but also highlight its potential to revolutionize active safety systems in AWD EVs. Through continuous learning and adaptation, the RL-based system promises enhanced stability and performance, paving the way for more intelligent experiences in the future.

## VI. CONCLUSION

A novel torque allocation method is introduced in this paper established on the DDPG algorithm in enhancing the dynamic stability and maneuverability of an AWD EV. The proposed algorithm exploits the LQR as the high-level controller, while the novel RL-based torque allocation method is utilized for the torque allocation. The integration of this advanced control strategy has proven to optimize torque distribution among the wheels, ensuring superior maneuverability and stability in comparison with the conventional model with the low-level average torque allocation method. The findings of this

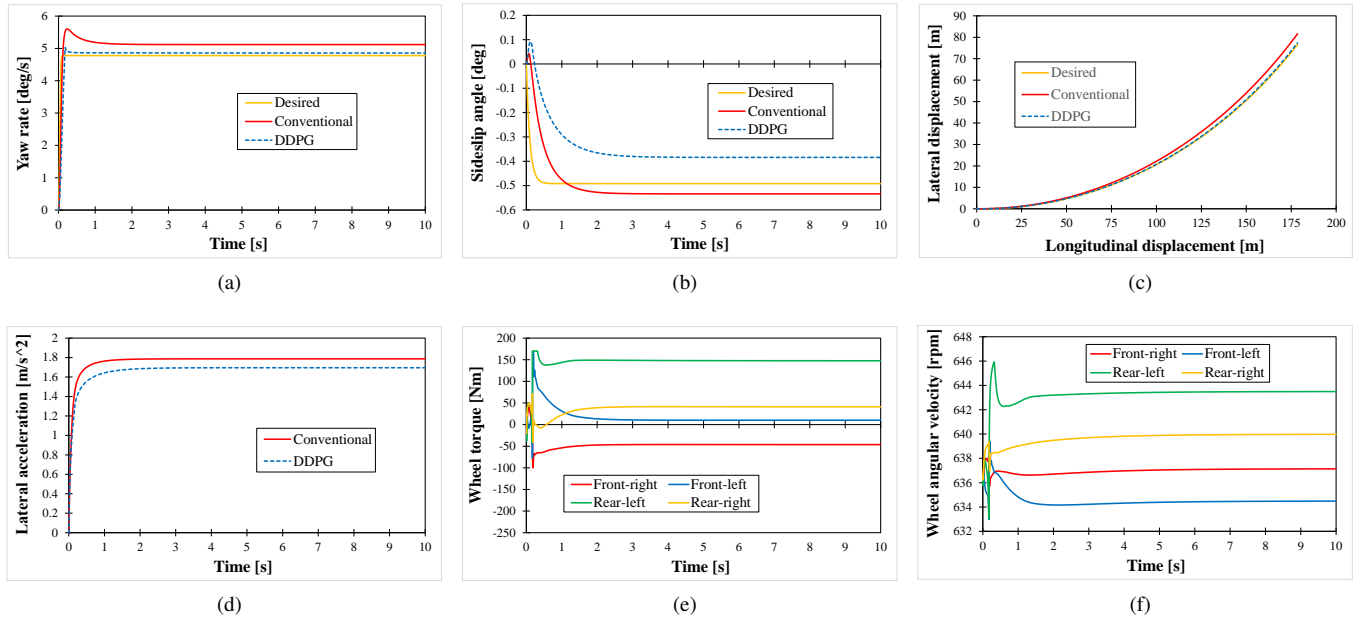


Fig. 5: Simulation results: (a) Yaw rate, (b) Sideslip angle, (c) Trajectory, (d) Lateral acceleration, (e) Wheel torques, (d) Wheel angular velocities

research verify the superior performance of the proposed DDPG algorithm through the reduced error of the yaw rate and sideslip angle, while the vehicle is capable of adhering to the intended path and avoiding understeer and oversteer.

#### REFERENCES

- [1] Ningyuan Guo, Basilio Lenzo, Xudong Zhang, Yuan Zou, Ruiqing Zhai, and Tao Zhang. A real-time nonlinear model predictive controller for yaw motion optimization of distributed drive electric vehicles. *IEEE Transactions on Vehicular Technology*, 69(5):4935–4946, 2020.
- [2] Matteo Dalboni, Gil Martins, Davide Tavernini, Umberto Montanaro, Alessandro Soldati, Carlo Concari, Miguel Dhaens, and Aldo Sorniotti. On the energy efficiency potential of multi-actuated electric vehicles. *IEEE Transactions on Vehicular Technology*, 2024.
- [3] Reza Jafari, Pedram Asef, Pouria Sarhadi, and Xiaozhe Pei. Optimal gear ratio selection of linear primary permanent magnet vernier machines for wave energy applications. *IET Renewable Power Generation*, 17(16):3856–3871, 2023.
- [4] Hao Chen and Chen Lv. Rhonn-modeling-based predictive safety assessment and torque vectoring for holistic stabilization of electrified vehicles. *IEEE/ASME Transactions on Mechatronics*, 28(1):450–460, 2022.
- [5] Hanghang Liu, Lin Zhang, Ping Wang, and Hong Chen. A real-time nmpe strategy for electric vehicle stability improvement combining torque vectoring with rear-wheel steering. *IEEE Transactions on Transportation Electrification*, 8(3):3825–3835, 2022.
- [6] Lei Wang, Hui Pang, Peng Wang, Minhao Liu, and Chuan Hu. A yaw stability-guaranteed hierarchical coordination control strategy for four-wheel drive electric vehicles using an unscented kalman filter. *Journal of the Franklin Institute*, 360(13):9663–9688, 2023.
- [7] Fadel Tarhini, Reine Talj, and Moustapha Doumiati. Dual-level control architectures for over-actuated autonomous vehicle’s stability, path-tracking, and energy economy. *IEEE Transactions on Intelligent Vehicles*, 2023.
- [8] Mansour Ataei, Amir Khajepour, and Soo Jeon. Model predictive control for integrated lateral stability, traction/braking control, and rollover prevention of electric vehicles. *Vehicle system dynamics*, 2019.
- [9] Alberto Parra, Asier Zubizarreta, Joshué Pérez, and Martín Dendaluce. Intelligent torque vectoring approach for electric vehicles with per-wheel motors. *Complexity*, 2018:1–14, 2018.
- [10] João Antunes, André Antunes, Pedro Outeiro, Carlos Cardeira, and Paulo Oliveira. Testing of a torque vectoring controller for a formula student prototype. *Robotics and Autonomous Systems*, 113:56–62, 2019.
- [11] Narjes Ahmadian, Alireza Khosravi, and Pouria Sarhadi. Driver assistant yaw stability control via integration of afs and dyc. *Vehicle system dynamics*, 60(5):1742–1762, 2022.
- [12] Narjes Ahmadian, Alireza Khosravi, and Pouria Sarhadi. Integrated model reference adaptive control to coordinate active front steering and direct yaw moment control. *ISA transactions*, 106:85–96, 2020.
- [13] Hongwei Wang, Jie Han, and Haotian Zhang. Lateral stability analysis of 4wd electric vehicle based on sliding mode control and optimal distribution torque strategy. In *Actuators*, volume 11, page 244. MDPI, 2022.
- [14] Huifan Deng, Youqun Zhao, Anh-Tu Nguyen, and Chao Huang. Fault-tolerant predictive control with deep-reinforcement-learning-based torque distribution for four in-wheel motor drive electric vehicles. *IEEE/ASME Transactions on Mechatronics*, 28(2):668–680, 2023.
- [15] Jinhao Liang, Jiwei Feng, Yanbo Lu, Guodong Yin, Weichao Zhuang, and Xiang Mao. A direct yaw moment control framework through robust ts fuzzy approach considering vehicle stability margin. *IEEE/ASME Transactions on Mechatronics*, 2023.
- [16] Xiaoqiang Sun, Yulin Wang, Yingfeng Cai, Pak Kin Wong, Long Chen, and Shaoyi Bei. Nonsingular terminal sliding mode based direct yaw moment control for four-wheel independently actuated autonomous vehicles. *IEEE Transactions on Transportation Electrification*, 2022.
- [17] Ningyuan Guo, Xudong Zhang, Yuan Zou, Basilio Lenzo, and Tao Zhang. A computationally efficient path-following control strategy of autonomous electric vehicles with yaw motion stabilization. *IEEE Transactions on Transportation Electrification*, 6(2):728–739, 2020.
- [18] Lie Guo, Zhenyu Tan, and Yijie Zhao. Real-time self-adjusting lqr method for autonomous vehicle lateral control. In *2023 7th CAA International Conference on Vehicular Control and Intelligence (CVCI)*, pages 1–6. IEEE, 2023.
- [19] Aria Noori Asiabar and Reza Kazemi. A direct yaw moment controller for a four in-wheel motor drive electric vehicle using adaptive sliding mode control. *Proceedings of the institution of mechanical engineers, part K: journal of multi-body dynamics*, 233(3):549–567, 2019.